GOSPODARKA SUROWCAMI MINERALNYMI – MINERAL RESOURCES MANAGEMENT

2025 Volume 41 Issue 1 Pages 123–139

DOI: 10.24425/gsm.2025.153171

DECAN ZENG[1], CHUNRONG PAN[2], KAI FENG[3], XIN LUO[4]

A novel magnetite ore refined sorting method based on magnetic induction and CNN-SK-BiLSTM network

Introduction

In modern industry, iron plays an indispensable role as a vital pillar material (Wang et al. 2023). However, Magnetite ore, one of the primary raw materials of iron, is a valuable non-renewable resource (Sahu et al 2022). Therefore, it is particularly urgent to improve the effective use of magnetite ore. The refined sorting of magnetite ore is no longer limited to the simple distinction between good and waste ore but is accurately sorted into several grades according to industrial needs. It not only helps to improve the quality of magnetite ore but also reduces the production of tailings, which contributes to the rational use of resources and the protection of the environment.

✉ Corresponding Author: Chunrong Pan; e-mail: crpan@jxust.edu.cn

[1] School of Mechanical and Electrical Engineering, Jiangxi University of Science and Technology, Ganzhou 341000, China; ORCID iD: 0009-0001-1605-2142; e-mail: 7120230090@mail.jxust.edu.cn

[2] School of Mechanical and Electrical Engineering, Jiangxi University of Science and Technology, Ganzhou 341000, China; e-mail: crpan@jxust.edu.cn

[3] School of Mechanical and Electrical Engineering, Jiangxi University of Science and Technology, Ganzhou 341000, China; e-mail: 7120230091@mail.jxust.edu.cn

[4] School of Mechanical and Electrical Engineering, Jiangxi University of Science and Technology, Ganzhou 341000, China; e-mail: 7120220001@mail.jxust.edu.cn

Nowadays, there exist three mainstream ore sorting methods based on optical sensors, X-ray sensors, and high-resolution cameras (Luo et al. 2022). The optical sensors are based on the properties of the ore to be reflected, absorbed, or transmitted in the spectral range for sorting. Reflectance spectroscopy has been successfully used to sort ores by some researchers (Fuentes et al. 2021; Nie et al. 2023; Wang et al. 2023; Xie et al. 2023). However, this detection method is only suitable for sorting between different ores, and it is not easy to detect the content of ore components. Its classification method distinguishes the detected spectral features of the ore by comparing them with the known spectral features. Hence, this method is not applicable to the refined sorting of magnetite ores. X-ray sensors can see through the ore and measure its chemical composition and density. Researchers have classified ores using X-ray transmission with satisfactory results (Henley et al. 2022; Kern et al. 2022; Zhang et al. 2024). However, this detection method is easily affected by other components or impurities in the ore, and in the fine sorting of magnetite ore, it needs to be combined with a variety of sensors or technologies to improve the accuracy and efficiency and is limited by the high cost of equipment and high radiation hazard, so this method is also not applicable to the sorting of magnetite ore. High-resolution cameras can capture high-resolution images of ores, and computer vision technology is used to analyze and identify the images and classify the ores based on their shape, texture, and other characteristics. By using computer vision, researchers have successfully achieved good results in ore sorting (Baraboshkin et al. 2020; Liu et al. 2021; Shatwell et al. 2023). This detection method can only identify the surface color, texture, and other features of the ore and cannot measure its composition.

Additionally, the deep learning classification algorithm based on high-definition ore images requires enormous data storage resources, which is not conducive to the deployment of the ore sorting site. Therefore, this method is not suitable for the refined sorting of magnetite ore. In summary, refined sorting of magnetite ores is limited by common ore sorting methods. As can be seen, the above ore sorting methods have limitations in the refined sorting of magnetite ores. Therefore, this paper proposes a new detection method for magnetite ore, taking into account the characteristics of internal magnetism of magnetite ore; the Hall sensor is used to collect its magnetic induction signal as it passes through an external magnetic field and generate a time-series data set. This allows the quantification of the magnetite content in the ore and provides training samples for deep-learning classification.

In recent times, deep learning techniques have been employed extensively across a range of industries due to their efficacy in feature extraction and classification. In the field of industrial manufacturing, some researchers employ deep neural networks to extract features from vibration signals, with the objective of diagnosing mechanical faults and providing the basis for intelligent equipment (Keshun et al. 2024a, b, 2025). In the field of agriculture, researchers have employed deep networks in tree planting and reforestation projects (Vinod et al. 2024), thereby providing a foundation for the advancement of smart agriculture. In the medical area, researchers have created time series datasets from electrocardiograms (ECGs)

(Cho et al. 2024) and electroencephalograms (EEGs) (Jafari et al. 2023; Wang et al. 2023) and fed them into deep neural networks in order to obtain meaningful diagnostic results. In the transport field, researchers have applied deep learning to the detection of foreign objects on roads (Chen et al. 2024) and the study of automatic driving (Chen et al. 2022), achieving positive outcomes and providing theoretical support for intelligent transport. This paper proposes a new classification algorithm for magnetite ore. A deep learning convolutional neural network (CNN) with an LSTM and a selective kernel (SK) attention mechanism (CNN-SK-BiLSTM) is constructed based on a constructed time series dataset. Specifically, CNN is used to extract the spatial features of the time series signals. In contrast, LSTM is used to capture the temporal features of the time sequence, and the SK attention mechanism enhances the feature extraction capability of the model. The proposed model successfully realizes the refined four classes of magnetite ore from a mine in Liaoning Province, China, and achieves a high accuracy rate of 99.44% in the experiment.

The rest of this paper is organized as follows. Section 1 introduces the methodology, including the detection method and classification algorithm. Section 2 presents the results and discussion. Finally, conclusions and outlook are given in the last Section.

1. Methodology

As illustrated in Figure 1, the magnetite ore refining sorting method, which is based on magnetic induction and a deep learning network, primarily comprises two components:

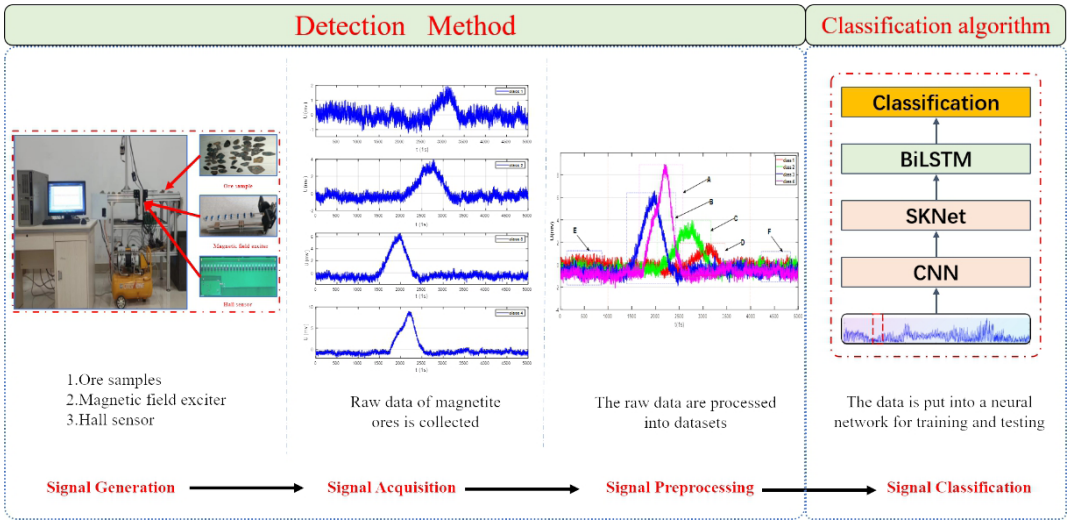

Fig. 1. The schematic diagram of refined sorting methodology, including the detection method and classification algorithm

Rys. 1. Schemat ideowy udoskonalonej metodologii sortowania z uwzględnieniem metody detekcji i algorytmu klasyfikacji

a detection method and a classification algorithm. The detection method comprises three steps:

1) generation of the magnetic induction signal of the ore through the exciter,
2) acquisition of the magnetic induction signal of the ore through the Hall sensor,
3) preprocessing of the magnetic induction signal to form a time series data set.

In contrast, the classification algorithm is a deep network comprising three components: the CNN module, the SK module, and the BiLSTM module. A substantial number of ore signals are employed to train and validate this model.

1.1. Refined sorting platform for magnetite ore

Figure 2 depicts a schematic representation of a magnetite ore sorting platform. The process comprises three principal stages. Initially, a magnetic induction signal is generated when the ore traverses an external magnetic field generated by permanent magnets. This signal is then detected by Hall sensors and conveyed to a computer, which subsequently applies a classification algorithm to categorize the signal. Finally, the computer transmits the classification signals to a pneumatic injection unit, which injects different classes of ore into distinct locations.

As illustrated in Figure 3, the magnetite ore is transported on a conveyor belt. An external magnetic field exciter, comprising neodymium-iron-boron (NdFeB) permanent magnets, is situated beneath the conveyor belt to generate a localized magnetic field. Hall sensors have also been installed in this region to capture the magnetic induction signals produced by the ore as it traverses the magnetic field area. These signals are then conveyed to a computer for further processing.

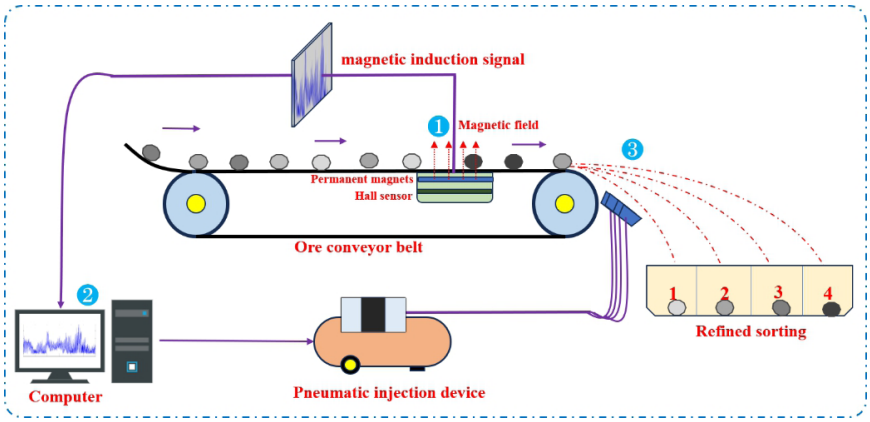

Fig. 2. Schematic diagram of the fine sorting process of magnetite ore, including the magnetic ore detection process, the sorting process and the pneumatic actuation process

Rys. 2. Schemat ideowy procesu drobnego sortowania rudy magnetytu z uwzględnieniem procesu magnetycznej detekcji rudy, procesu sortowania oraz procesu uruchamiania pneumatycznego

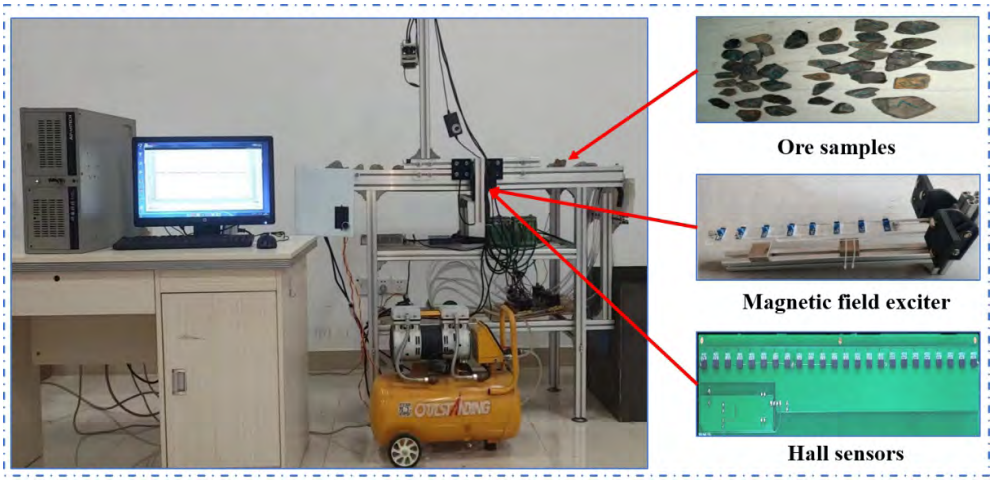

Fig. 3. Ore magnetic induction signal acquisition experiment platform, including external magnetic field exciter, Hall sensor, computer

Rys. 3. Platforma do eksperymentów akwizycji sygnału indukcji magnetycznej rudy, zawierająca zewnętrzny wzbudnik pola magnetycznego, czujnik Halla i komputer

1.2. Detection method based on magnetic induction

1.2.1. Raw data acquisition

The magnetite ores utilized in this study were sourced from a mine in Liaoning Province, China. The magnetite ores, which ranged in size from 10 to 40 mm, were selected at random for testing. The greater the quantity of iron tetraoxide (Fe_3O_4) present within the ore, the more pronounced the magnetic induction signal produced upon traversing an external magnetic field generated by a permanent magnet. The ore samples were classified into four categories, designated as Classes 1 to 4, based on their Fe tetraoxide (Fe_3O_4) content and the strength of the magnetic induction signal. During the experiment, the time allocated for each ore to traverse the experimental acquisition platform was fixed at one second, while the sampling rate of the data acquisition card was set at 5 kHz. Consequently, each signal sample comprised 5,000 data points. The speed of the conveyor belt was set to 0.1 m/s. Furthermore, the data acquisition software on the operational computer generates the acquired magnetic induction signal waveforms in real time. The raw data for all ore samples was successfully acquired through the repetition of the experiment. The waveforms of the collected source data for the four types of ores are illustrated in Figure 4.

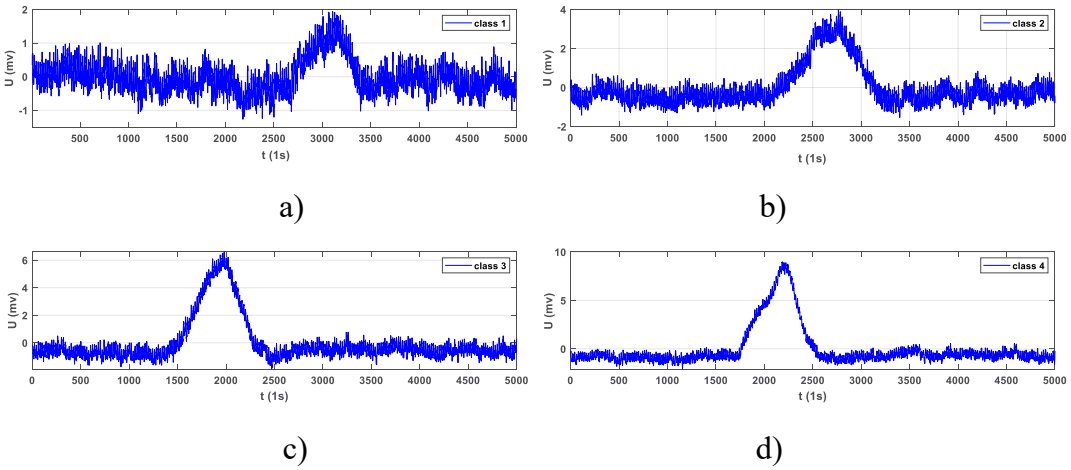

Fig. 4. Raw time-series signals
a–d are magnetic induction signals from classes 1–4 magnetite ores

Rys. 4. Surowe sygnały szeregów czasowych
a–d są sygnałami indukcji magnetycznej z rud magnetytu klas 1–4

1.2.2. Data preprocessing

During the course of the experiment, magnetic induction waveforms are generated by the ore samples as they traverse the external magnetic field. Figure 5 illustrates the waveforms of ore classes 1–4 in boxes A, B, C, and D, which exhibit distinct distributions. Furthermore, negligible signals are discernible in each source data set, as illustrated by E and F in the figure. To enhance the training process and optimize the utilization of computational

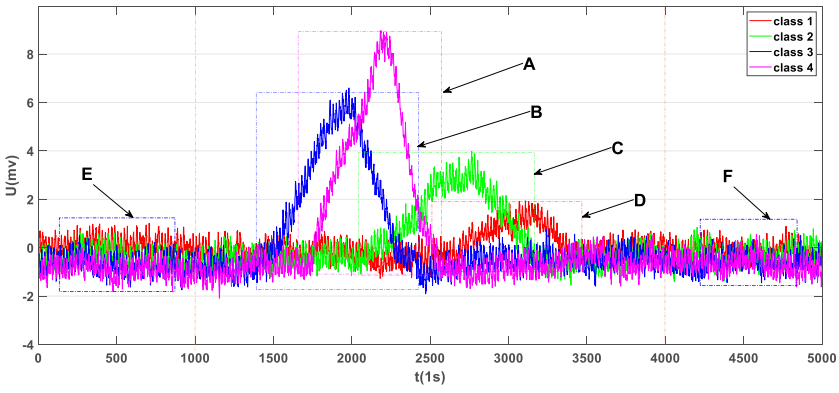

Fig. 5. Magnetic induction waveforms of four classes of ore samples

Rys. 5. Przebiegi indukcji magnetycznej czterech klas próbek rudy

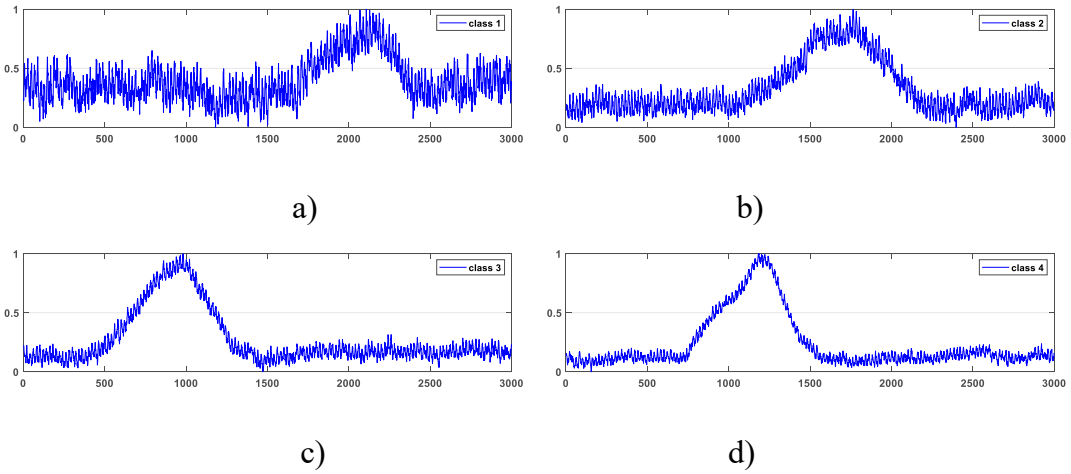

Fig. 6. Preprocessed time-series signals
a–d are magnetic induction signals from classes 1–4 magnetite ores

Rys. 6. Wstępnie przetworzone sygnały szeregów czasowych
a–d to sygnały indukcji magnetycznej z rud magnetytu klas 1–4

resources, invalid data were excluded, and only the 3,000 data points that contained pertinent feature signals were retained. In order to enhance the precision of the training process, the data underwent normalization without any alteration to its distribution, and was then mapped onto the interval [0,1]. The resulting signals are illustrated in Figure 6a–d. A total of 1,250 raw data signals were processed individually, with any unsuitable data resulting from experimental operations removed. This process yielded 1,200 samples, which were then combined to form the dataset, comprising 300 samples for each class and divided into training, validation, and testing sets in the ratio of 0.7:0.15:0.15.

1.3. Classification algorithm based on CNN-SK-BiLSTM network

The magnetic induction signal of ore exhibits irregularity and non-repeatability, rendering its features challenging to extract. To address this, a CNN network is utilized to extract the spatial features of the signals, while an LSTM network is employed to extract the temporal features (Xu et al. 2023). Additionally, an SK mechanism was introduced to enhance the model's ability to extract multi-scale features (Li et al. 2019), leading to the proposal of a CNN-SK-BiLSTM model.

As illustrated in Figure 7, the CNN network is a wide kernel convolutional neural network (Zhang et al. 2017) increasing the efficiency of fault diagnosis. Deep learning models can improve the accuracy of intelligent fault diagnosis with the help of their multilayer nonlinear

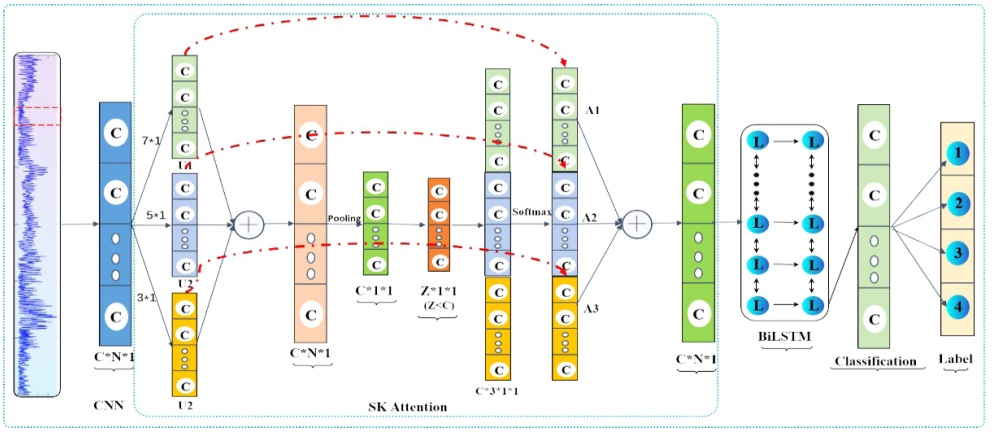

Fig. 7. Structure of the proposed model, including CNN module, SK attention module, BiLSTM module, and Classification module

Rys. 7. Struktura proponowanego modelu z uwzględnieniem modułu CNN, modułu uwagi SK, modułu BiLSTM i modułu klasyfikacji

Table 1. CNN-SK-BILSTM Model

Tabela 1. Model CNN-SK-BILSTM

CNN Module		
	conv2d([32,1], 16) ReluLayer	
SK Attention Module		
conv2d ([3,1], 64) ReluLayer	conv2d([5,1], 64) ReluLayer	conv2d([7,1], 64) ReluLayer
	additionLayer(3)	
	globalAveragePooling2dLayer	
	fullyConnectedLayer(16)	
fullyConnectedLayer(64)	fullyConnectedLayer(64)	fullyConnectedLayer(64)
sigmoidLayer		
multiplicationLayer	multiplicationLayer	multiplicationLayer
	additionLayer(3)	
BiLSTM Module		
	flattenLayer	
	bilstmLayer(32)	
	bilstmLayer(16)	
Classification Module		
	fullyConnectedLayer(4) softmaxLayer classificationLayer	

mapping ability. This paper proposes a novel method named Deep Convolutional Neural Networks with Wide First-layer Kernels (WDCNN, which mitigates the impact of certain high-frequency signals and enhances the model's generalizability. The attention mechanism is then divided into three steps (Jia et al. 2024):

1. Segmentation: This step performs multi-scale feature extraction on the signal by three convolutional kernels with different sizes, specifically 3×1, 5×1, and 7×1, respectively.
2. Fusion: This step first fuses the multi-features into one-dimensional vectors by global average pooling and then converts the features into Z×1×1 (Z < C) vectors by a fully connected layer.
3. Selection: In this phase, the features are initially reduced to C×1×1 vectors and then merged through the use of three fully connected layers.

Subsequently, the attention weights at varying scales are derived through a sigmoid layer and integrated with the original features of each branch. The BiLSTM module represents a bidirectional LSTM with exemplary feature extraction capabilities for time series signals (Yi and Bian 2021). The final module is the classifier, which receives the feature input and completes the classification. The parameters of the entire network are presented in Table 1.

2. Results and discussion

2.1. Evaluation indexes

Since magnetite selection is a four- classification problem, an evaluation index commonly used in classification, including accuracy, precision, recall, and F1 score, was used to measure the effectiveness and robustness of our model from different perspectives (Carrington et al. 2023).

$$Accuracy = \frac{TP + TN}{TP + FP + TN + FN} \tag{1}$$

$$Precision = \frac{TP}{TP + FP} \tag{2}$$

$$Recall = \frac{TP}{TP + FN} \tag{3}$$

$$F1 = \frac{2 \cdot Precision \cdot Recall}{Precision + Recall} \tag{4}$$

- *TP* – (true positive) is correctly classified as positive samples,
- *FP* – (false positive) is misclassified as positive samples,
- *TN* – (true negative) is correctly classified as negative samples,
- *FN* – (false negative) is misclassified as negative samples.

2.2. Experimental results of the proposed model

Figure 8 shows the accuracies of the 10 trials and the results show that all of the trainings achieved 100% accuracy, while the average accuracy of the tests was 98.45%, with a minimum of 97.22% and a maximum of 99.44%.

Table 2 shows the average accuracy, precision, recall and F1_Score value of the proposed CNN-SK – BiLSTM over 10 repeated runs, the average accuracy of all four categories exceeds 97% and exceeds 99 % for class 1 and 4, and the F1_Score value of all the detections exceeds 95%.

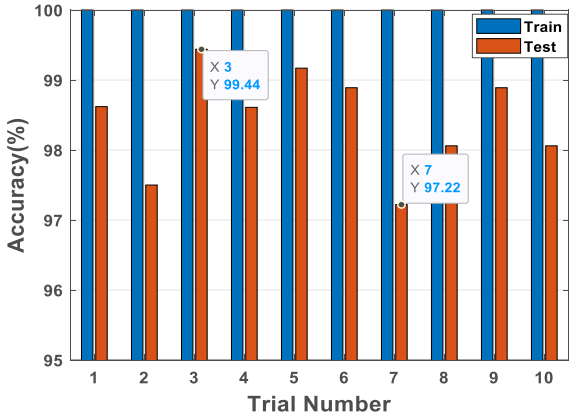

Fig. 8. Results of 10 trials of the proposed model

Rys. 8. Wyniki 10 prób zaproponowanego modelu

Table 2. Evaluation indexes for ten experiments of the proposed model

Tabela 2. Wskaźniki oceny dziesięciu eksperymentów proponowanego modelu

Class	Accuracy	Precision	Recall	F1_Score
1	99.00	99.54	96.31	97.85
2	97.83	94.64	96.90	95.71
3	97.89	95.76	95.91	95.77
4	99.06	97.93	98.51	98.19

Figure 9 shows the confusion matrix for the highest and lowest accuracy results (99.44% and 97.22%), where figure a is mainly the lower accuracy of class 2 with six samples misclassified as class 3, class 1 with two samples misclassified as class 2, class 3 with two samples misclassified as class 4, and class 4 with 100% accuracy in the test. Whereas in the most accurate test, classes 1 and 2 were both 100% accurate, only class 3 had 1 sample misclassified as class 2, and class 4 had 1 sample misclassified as class 1.

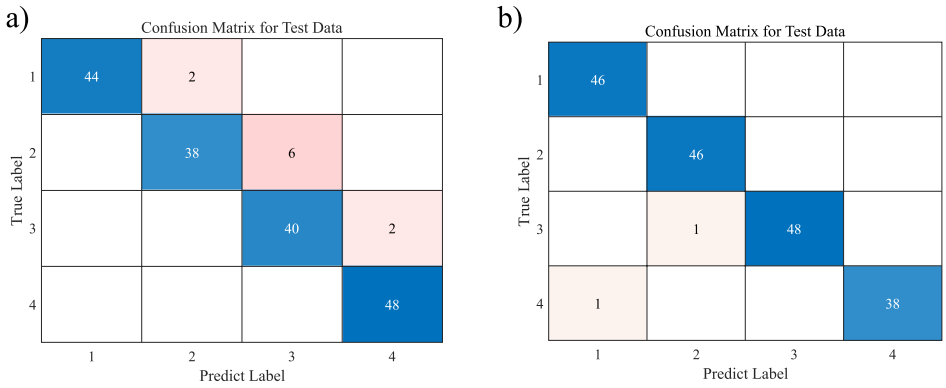

Fig. 9. Confusion matrix of the classification for CNN-SK-BiLSTM
a) highest accuracy = 99.44%, b) lowest accuracy = 97.22%

Rys. 9. Macierz zamieszania klasyfikacji dla CNN-SK-BiLSTM
a) najwyższa dokładność = 99,44%, b) najniższa dokładność = 97,22%

2.3. Comparative experiments with classical networks

To validate the superiority of the model proposed in this study, a series of training exercises were conducted on a number of different models, including the CNN model (Zhang et al 2017), MSCNN model (Chen et al. 2021; Roy and Todorovic 2016), SE-CNN model (Wang et al. 2019), LSTM model (Yu et al. 2019), and CNN-LSTM model (Kim and Cho 2019), along with CNN-SE-BiLSTM model (Rifaat et al. 2022; Hu et al. 2018). The evaluation metrics used for comparing the training results, as shown in Figure 10, encompass accuracy, precision, recall, and F1 score.

Ten independent experiments were conducted for each model, and the mean value of the metrics was calculated. To obtain a more comprehensive pairing, the accuracy, precision, recall, and F1 score for each label were enumerated. The following table presents the results of the experiments conducted for each model.

From the data presented in Figure 10, a number of inferences can be drawn.

1. The average accuracy of the hybrid CNN-LSTM model is 92.96%, which is superior to the independent CNN (92.31%) and BiLSTM (90.19%) models. Therefore, it is essential to implement a hybrid design for the model.

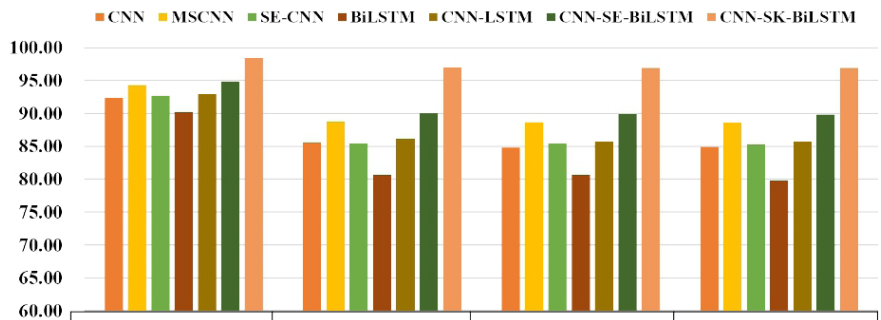

	Accuracy(%)	Precision(%)	Recall(%)	F1_Score(%)
CNN	92.31	85.65	84.84	84.86
MSCNN	94.35	88.74	88.65	88.60
SE-CNN	92.73	85.45	85.42	85.22
BiLSTM	90.19	80.67	80.71	79.74
CNN-LSTM	92.96	86.12	85.70	85.66
CNN-SE-BiLSTM	94.88	90.01	89.95	89.83
CNN-SK-BiLSTM	98.45	96.97	96.91	96.88

Fig. 10. Performance comparison of CNN-SK-BiLSTM with other classic networks in our dataset

Rys. 10. Porównanie wydajności CNN-SK-BiLSTM z innymi klasycznymi sieciami w naszym zbiorze danych

2. The accuracy of MSCNN (94.35%) is 2.04% higher than that of CNN (92.31%), and the average accuracy of SE-CNN (92.73%) is also higher than that of simple CNN (92.31%), indicating that the improvement of the model with multiscale and an increasing attention mechanism can contribute to enhancing the accuracy of the model.
3. A comparison of the CNN-SE-BiLSTM model with the CNN-SK-BiLSTM model reveals that the latter exhibits superior performance, with an accuracy of 3.57% higher, a precision of 6.96% higher, a recall of 6.96% higher, and an F1 score that is 7.05% higher.

This suggests that the multiscale attention mechanism is more effective. In conclusion, this paper proposes the CNN-SK-BiLSTM hybrid model with a multiscale attention mechanism as an effective algorithm for magnetite ore refined sorting.

The T-SNE algorithm (van der Maaten and Hinton 2008) is a non-linear technique for reducing high-dimensional data to low dimensions. It enables data visualization and can be employed to evaluate the success of neural network feature extraction. In Figure 11, different colored points represent different classes of magnetite. Points that are closer to the same class and further away from other classes indicate better classification. Figure 10a shows the visual analysis of the raw input data, which shows that the points of different classes are clustered together and difficult to classify. Figures 11b–h show the visual analysis of the final output features of each model based on the T-SNE algorithm. The original chaotic input features are classified to different degrees after feature extraction by each method. According to the comparison of Figure 11b–h, the various clusters' boundaries under the

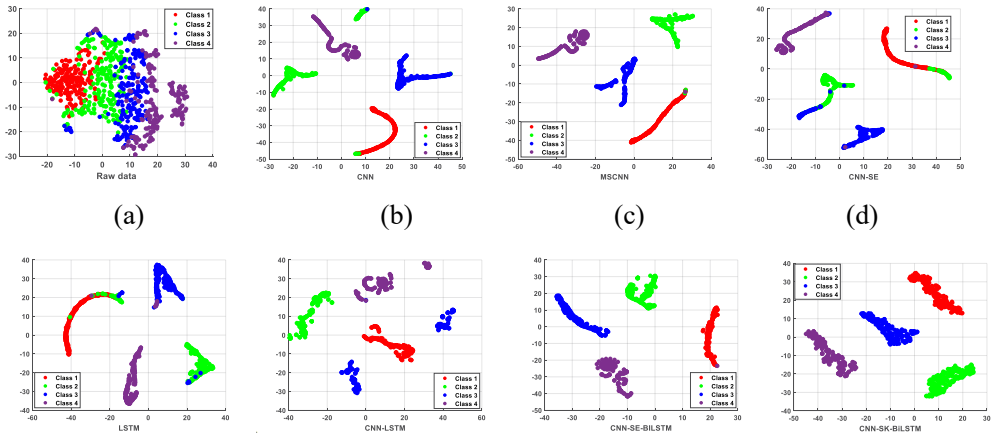

Fig. 11. T-SNE analysis diagram
a) Raw data, b) CNN, c) MSCNN, d) CNN-SE, e) LSTM, f) CNN-LSTM,
g) CNN-SE-BiLSTM, h) CNN-SK-BiLSTM

Rys. 11. Schemat analizy T-SNE
a) Surowe dane, b) CNN, c) MSCNN, d) CNN-SE, e) LSTM, f) CNN-LSTM,
g) CNN-SE-BiLSTM, h) CNN-SK-BiLSTM

CNN-SE-BiLSTM method and the CNN-SK-BiLSTM method are more evident than the other methods. The CNN-SK-BiLSTM method has fewer error points close to the clusters of different classes compared to CNN-SE-BiLSTM. Making it possible to conclude that CNN-SK-BiLSTM has the best classification results.

Conclusion

The refined sorting of magnetite resources is a crucial step in optimizing their utilization. However, the conventional ore sorting methods that have been employed have not been able to achieve this goal. In this paper, an innovative detection method is presented, which employs an external magnetic field to excite and collect the magnetic induction information of magnetite ores. This method is designed to exploit the natural magnetic properties of these ores. A deep learning model with a multi-scale attention mechanism, CNN-SK-BiLSTM, is proposed, combining the specific good feature extraction and classification capabilities of deep learning techniques. The model was successfully tested on magnetite ore from a mine in Liaoning Province, China, and the ore was refined into four categories. The proposed model achieved the highest accuracy of 99.44% in the experiments, as well as the desired precision, recall, and F1 score. Furthermore, comparative experiments were conducted between the proposed model and other popular models, the results of which demonstrated

that the performance of the proposed model was markedly superior to that of the other models. The findings presented in this paper provide a foundation for the advancement of engineering techniques for the sorting of magnetite ore, which is crucial for enhancing the utilization of resources.

Although the proposed method in this paper is effective in detecting magnetite ores and the depth model is adept at classification, two issues persist in the deployment of deep learning in engineering applications. The first is that the number of parameters and operations within the depth model is substantial, making it challenging to implement edge equipment in mining environments. The second is that the interpretability of the depth model is limited, which hinders the advancement of theoretical research in this field. Further progress will be made by continuing research in these two areas, which will provide additional valuable results for the field of mining engineering.

This work was supported in part by the Science and Technology Research Project GJJ2203618, 2022, Department of Education of Jiangxi Province and the Special Project for Postgraduate Innovation of Jiangxi Province (YC2021-S577).

The Authors have no conflict of interest to declare.

The data that has been used is confidential.

REFERENCES

Baraboshkin et al. 2020 – Baraboshkin, E.E., Ismailova, L.S., Orlov, D.M., Zhukovskaya, E.A., Kalmykov, G.A., Khotylev, O.V., Baraboshkin, E.Y. and Koroteev, D.A. 2020. Deep convolutions for in-depth automated rock typing. *Computers & Geosciences* 135, DOI: 10.1016/j.cageo.2019.104330.

Chen et al. 2021 – Chen, X., Zhang, B., and Gao, D. 2021. Bearing fault diagnosis base on multi-scale CNN and LSTM model. *Journal of Intelligent Manufacturing* 32(4), pp. 971–987, DOI: 10.1007/s10845-020-01600-2.

Chen et al. 2022 – Chen, Z., Guo, H., Yang, J., Jiao, H., Feng, Z., Chen, L. and Gao, T. 2022. Fast vehicle detection algorithm in traffic scene based on improved SSD. *Measurement* 201, DOI: 10.1016/j.measurement.2022.111655.

Chen et al. 2024 – Chen, Z., Yang, J., Feng, Z. and Zhu, H. 2024. RailFOD23: A dataset for foreign object detection on railroad transmission lines. *Scientific Data* 11(1), DOI: 10.1038/s41597-024-02918-9.

Cho et al. 2024 – Cho, H.M., Han, S., Seong, J.K. and Youn, I. 2024. Deep learning-based dynamic ventilatory threshold estimation from electrocardiograms. *Comput Methods Programs Biomed.*, DOI: 10.1016/j.cmpb.2023.107973.

Fuentes et al. 2021 – Fuentes, R., Luarte, D., Sandoval, C., Myakalwar, A.K., Yáñez, J. and Sbarbaro, D. 2021. Data fusion of Laser Induced Breakdown Spectroscopy and Diffuse Reflectance for improved analysis of mineral species in copper concentrates. *Minerals Engineering* 173(12), DOI: 10.1016/j.mineng.2021.107193.

Henley et al. 2022 – Henley, R.W., Mernagh, T., Leys, C., Troitzsch, U., Bevitt, J., Brink, F., Gardner, J., Knuefing, L., Wheeler, J., Limaye, A., Turner, M. and Zhang, Y. 2022. Potassium silicate alteration in porphyry copper-gold deposits: a case study at the giant maar-diatreme hosted Grasberg deposit, Indonesia. *Journal of Volcanology and Geothermal Research* 432, DOI: 10.1016/j.jvolgeores.2022.107710.

Hu et al. 2018 – Hu, J., Shen, L. and Sun, G. 2018. Squeeze-and-excitation networks. *IEEE/CVF Conference on Computer Vision and Pattern Recognition (CVPR)*, pp. 7132–7141.

Jafari et al. 2023 – Jafari, M., Shoeibi, A., Khodatars, M., Bagherzadeh, S., Shalbaf, A., García, D.L., Gorriz, J.M. and Acharya, U.R. 2023. Emotion recognition in EEG signals using deep learning methods: A review. *Computers in Biology and Medicine* 165, DOI: 10.1016/j.compbiomed.2023.107450.

Jia et al. 2024 – Jia, C., Long, M. and Liu, Y. 2024. Enhanced face morphing attack detection using error-level analysis and efficient selective kernel network. *Computers & Security* 137, DOI: 10.1016/j.cose.2023.103640.

Kern et al. 2022 – Kern, M., Akushika, J.N.P., Godinho, J.R.A., Schmiedel, T. and Gutzmer, J. 2022. Integration of X-ray radiography and automated mineralogy data for the optimization of ore sorting routines. *Minerals Engineering* 186, DOI: 10.1016/j.mineng.2022.107739.

Keshun et al. 2024a – Keshun, Y., Zengwei, L. and Yingkui, G. 2024a. A performance-interpretable intelligent fusion of sound and vibration signals for bearing fault diagnosis via dynamic CAME. *Nonlinear Dynamics* 112(23), pp. 20903–20940, DOI: 10.1007/s11071-024-10157-1.

Keshun et al. 2024b –Keshun, Y., Puzhou, W. and Yingkui, G. 2024b. Toward Efficient and Interpretative Rolling Bearing Fault Diagnosis via Quadratic Neural Network With Bi-LSTM. *IEEE Internet of Things Journal* 11(13), pp. 23002–23019, DOI: 10.1109/JIOT.2024.3377731.

Keshun et al. 2025 –Keshun, Y., Puzhou, W. and Yingkui, G. 2025. A sound-vibration physical-information fusion constraint-guided deep learning method for rolling bearing fault diagnosis. *Reliability Engineering & System Safety* 253, DOI: 10.1016/j.ress.2024.110556.

Kim, T.Y. and Cho, S.-B. 2019. Predicting residential energy consumption using CNN-LSTM neural networks. *Energy* 182, pp. 72–81, 2019, DOI: 10.1016/j.energy.2019.05.230.

Li et al. 2019 – Li, X., Wang, W., Hu, X. and Yang, J. 2019. Selective kernel networks. *Proceedings of the IEEE/CVF conference on computer vision and pattern recognition*, pp. 510–519, DOI: 10.48550/arXiv.1903.06586.

Liu et al. 2021 – Liu, Y., Zhang, Z., Liu, X., Wang, L. and Xia, X. 2021. Performance evaluation of a deep learning based wet coal image classification. *Minerals Engineering* 171, DOI: 10.1016/j.mineng.2021.107126.

Luo et al. 2022 – Luo, X., He, K., Zhang, Y., He, P. and Zhang, Y. 2022.A review of intelligent ore sorting technology and equipment development. *International Journal of Minerals Metallurgy and Materials* 29(9), pp. 1647––1655, DOI: 10.1007/s12613-022-2477-5.

van der Maaten L. and Hinton, G. 2008. Visualizing Data using t-SNE. *Journal of Machine Learning Research* 9, pp. 2579–2605.

Nie et al. 2023 – Nie, C., Jiang, J., Deng, J., Li, K., Jia, L. and Sun, T. 2023. Predicting TFe content and sorting iron ores from hyperspectral image by variational mode decomposition-based spectral feature. *Journal of Cleaner Production* 429, DOI: 10.1016/j.jclepro.2023.139629.

Rifaat et al. 2022 – Rifaat, N, Ghosh, U.K. and Sayeed, A. 2022. Accurate gait recognition with inertial sensors using a new FCN-BiLSTM architecture. *Computers and Electrical Engineering* 104, DOI: 10.1016/j.compeleceng.2022.108428.

Roy, A. and Todorovic, S. 2016. A multi-scale cnn for affordance segmentation in rgb images. *European Conference on Computer Vision – ECCV 2016*, pp. 186–201, DOI: 10.1007/978-3-319-46493-0_12.

Sahu et al. 2022 – Sahu, S.N. Meikap, B.C. and Biswal, S.K., 'Magnetization roasting of waste iron ore beneficiation plant tailings using sawdust biomass; A novel approach to produce metallurgical grade pellets. *Journal of Cleaner Production* 343, DOI: 10.1016/j.jclepro.2022.130894.

Shatwellet al. 2023 – Shatwell, D.G., Murray, V. and Barton, A. 2023. Real-time ore sorting using color and texture analysis. *International Journal of Mining Science and Technology* 33(6), pp. 659–674, DOI: 10.1016/j.ijmst.2023.03.004.

Vinod et al. 2024 – Vinod, P., Behera, M., Jaya Prakash, A., Hebbar, R. and Srivastav, S. 2024. A novel multitask transformer deep learning architecture for joint classification and segmentation of horticulture plantations using very High-Resolution satellite imagery. *Computers and Electronics in Agriculture* 227, DOI: 10.1016/j.compag.2024.109540.

Wang et al. 2019 – Wang, H., Xu, J., Yan, R. and Gao, R.X. 2019. A new intelligent bearing fault diagnosis method using SDP representation and SE-CNN. *IEEE Transactions on Instrumentation and Measurement* 69(5), pp. 2377–2389, DOI: 10.1109/TIM.2019.2956332.

Wang et al. 2022 – Wang, Q., Xiao, J., Li, Y., Lu, Y., Jinjia Guo, J., Tian, Y. and Ren, L. 2022. Mid-level data fusion of Raman spectroscopy and laser-induced breakdown spectroscopy: Improving ores identification accuracy. *Analytica Chimica Acta* 1240, DOI: 10.1016/j.aca.2022.340772.

Wang et al. 2023 – Wang, C., Walsh, S.D.C., Weng, Z., Haynes, M.W., Summerfield, D. and Feitz, A. 2023. Green steel: Synergies between the Australian iron ore industry and the production of green hydrogen. *International Journal of Hydrogen Energy* 48(10), pp. 32277–32293, DOI: 10.1016/j.ijhydene.2023.05.041.

Wang et al. 2023 – Wang, X., Liesaputra, V., Liu, Z., Wang, Y. and Huang, Z. 2023. An in-depth survey on Deep Learning-based Motor Imagery Electroencephalogram (EEG) classification. *Artificial Intelligence in Medicine* 147, DOI: 10.1016/j.artmed.2023.102738.

Xie et al. 2023 – Xie, H., Mao, Z., Xiao, D., and Li, Z. 2023. Rapid detection of molybdenum ore grade based on visible-infrared spectroscopy and MTSVD-TGJO-ELM. *Spectrochimica Acta Part A: Molecular and Biomolecular Spectroscopy* 298, DOI: 10.1016/j.saa.2023.122789.

Xu et al. 2023 – Xu, C., Liang, R., Wu, X., Cao, C., Chen, J., Yang, C., Zhou, Y., Wen, T., Lv, H. and Wei, C. 2023. A Hybrid Model Integrating CNN–BiLSTM and CBAM for Anchor Damage Events Recognition of Submarine Cables. *IEEE Transactions on Instrumentation and Measurement* 72, pp. 1–11, DOI: 10.1109/TIM.2023.3290323.

Yi Y. and Bian, Y. 2021. Named Entity Recognition with Gating Mechanism and Parallel BiLSTM. *Journal of Web Engineering* 20(4), pp. 1219–1238, DOI: 10.13052/jwe1540-9589.20413.

Yu et al. 2019 – Yu, Y., Si, X., Hu, C. and Zhang, J. 2019. A review of recurrent neural networks: LSTM cells and network architectures. *Neural Computation* 31(7), pp. 1235–1270, DOI: 10.1162/neco_a_01199.

Zhang et al. 2017 – Zhang, W., Peng, G., Li, C., Chen, Y. and Zhang, Z. 2017. A New Deep Learning Model for Fault Diagnosis with Good Anti-Noise and Domain Adaptation Ability on Raw Vibration Signals. *Sensors* 17(3), DOI: 10.3390/s17020425.

Zhang et al. 2024 – Zhang, Y., Francois, N., Henley, R., Turner, M., Saadatfar, M., Brink, F.J. and Knackstedt, M. 2024. In-situ study of texture-breakage coupling in a copper ore using X-ray micro-CT. *Minerals Engineering* 205, DOI: 10.1016/j.mineng.2023.108464.

A NOVEL MAGNETITE ORE REFINED SORTING METHOD BASED ON MAGNETIC INDUCTION AND CNN-SK-BILSTM NETWORK

Keywords

ore sorting, magnetite induction, deep learning, attention

Abstract

Magnetite ore is a non-renewable resource that needs to be utilized effectively. Refined sorting of magnetite ore is not simply sorting it into good ore or waste ore but finely sorting it into different grades due to its magnetite content, which not only helps to improve its utilization but also reduces the energy consumption of the following process. However, traditional ore sorting methods based on optical sensors, X-ray sensors, and high-resolution cameras are challenging to achieve refined sorting for magnetite ores because of the limitations of their respective detection methods and classification algorithms. To this end, a new detection method for magnetite content is proposed in this paper; the magnetic induction signal of magnetite ore when it passes through an external magnetic field is captured by Hall sensors and made into a quantifiable time-series dataset. Meanwhile, a deep learning classification algorithm CNN-SK-BiLSTM with a multi-scale attention mechanism is proposed, which successfully sorts magnetite ore from a mine in Liaoning Province, China, into four classes finely. The experimental results show that the accuracy of the model is up to 99.44%, and the precision, recall,

and F1 scores are acceptable. In addition, comparative experiments between the proposed model and other standard models were conducted. The results show that the performance of the proposed model is significantly better than the others. This paper provides ideas for the study of refined sorting of magnetite ore.

NOWATORSKA METODA SORTOWANIA RAFINOWANEJ RUDY MAGNETYTU OPARTA NA INDUKCJI MAGNETYCZNEJ I SIECI CNN-SK-BILSTM

Słowa kluczowe

sortowanie rud, indukcja magnetytu, głębokie uczenie się, uwaga

Streszczenie

Ruda magnetytu jest zasobem nieodnawialnym, który należy efektywnie wykorzystać. Rafinowane sortowanie rudy magnetytu nie polega po prostu na sortowaniu jej na dobrą rudę lub rudę odpadową, ale na dokładnym sortowaniu na różne gatunki ze względu na zawartość magnetytu, co nie tylko pomaga poprawić jej wykorzystanie, ale także zmniejsza zużycie energii w kolejnym procesie. Jednak tradycyjne metody sortowania rud oparte na czujnikach optycznych, czujnikach rentgenowskich i kamerach o wysokiej rozdzielczości stanowią wyzwanie w celu uzyskania udoskonalonego sortowania rud magnetytu ze względu na ograniczenia odpowiednich metod wykrywania i algorytmów klasyfikacji. W tym celu w artykule zaproponowano nową metodę wykrywania zawartości magnetytu. Sygnał indukcji magnetycznej rudy magnetytu przechodzącej przez zewnętrzne pole magnetyczne jest wychwytywany przez czujniki Halla i przekształcany w wymierny zbiór danych w formie szeregów czasowych. Tymczasem zaproponowano algorytm klasyfikacji głębokiego uczenia się CNN-SK-BiLSTM z wieloskalowym mechanizmem uwagi, który z powodzeniem sortuje rudę magnetytu z kopalni w prowincji Liaoning w Chinach na cztery klasy. Wyniki eksperymentów pokazują, że dokładność modelu sięga 99,44%, a precyzja, powtarzalność i wyniki F1 są akceptowalne. Dodatkowo przeprowadzono eksperymenty porównawcze zaproponowanego modelu z innymi modelami standardowymi. Wyniki pokazują, że wydajność proponowanego modelu jest znacznie lepsza od pozostałych. W artykule przedstawiono pomysły na badania rafinowanego sortowania rudy magnetytu.